Title

Assembly and seasonality of core phyllosphere microbiota on perennial biofuel crops

Authors

Keara L Grady[1,2,a], Jackson W. Sorensen[1,2,a], Nejc Stopnisek[2,3,a], John Guittar[1,4], and Ashley Shade[1,2,3,5,6]*

1. Department of Microbiology and Molecular Genetics, Michigan State University, East Lansing MI 48840 USA
2. The DOE Great Lakes Bioenergy Research Center, Michigan State University, East Lansing, MI 48840
3. Program in Ecology, Evolutionary Biology and Behavior, Michigan State University, East Lansing MI 48840
4. Kellogg Biological Station, Michigan State University, Hickory Corners, MI 43060
5. The Plant Resilience Institute, Michigan State University, East Lansing MI 48840
6. Department of Plant, Soil and Microbial Sciences, Michigan State University, East Lansing MI 48840

[a]Contributed equally

*correspondence, shadeash@msu.edu

Keywords

Miscanthus, switchgrass, temporal dynamics, microbiome, agroecosystems, bioenergy, sustainability, plant-microbe interactions, leaf, phytobiome

Abstract

Perennial grasses are promising feedstocks for biofuel production, and there is potential to leverage their native microbiomes to increase their productivity and resilience to environmental stress. Here, we characterize the 16S rRNA gene diversity and seasonal assembly of bacterial and archaeal microbiomes of two perennial cellulosic feedstocks, switchgrass (Panicum virgatum L.) and miscanthus (Miscanthus x giganteus). We sampled leaves and soil every three weeks from pre-emergence through senescence for two consecutive switchgrass growing seasons and one miscanthus season, and identified core leaf taxa based on abundance and occupancy. Virtually all leaf taxa are also detected in soil; source-sink modeling shows non-random, ecological filtering by the leaf, suggesting that soil is important reservoir of phyllosphere diversity. Core leaf taxa include early, mid, and late season groups that were consistent across years and crops. This consistency in leaf microbiome dynamics and core members is promising for microbiome manipulation or management to support biofuel crop production.

The phyllosphere (aerial parts of plants) represents the largest environmental surface area of microbial habitation on the planet [1–3], and much of that surface area is cultivated agriculture, including an estimated 1.5 x 10^7 km^2 of cropland [4]. Phyllosphere microorganisms may provide numerous benefits to plants, including increased stress tolerance [5–7], promotion of growth and reproduction [8–10], protection from foliar pathogens [11], and, with soil microbes, control of flowering phenology [12]. Phyllosphere microorganisms are also thought to play important roles in Earth's biogeochemical cycles by moderating methanol emissions from plants [13,14] and contributing to global nitrogen fixation [15]. Despite this importance, knowledge

of phyllosphere microbiomes remains relatively modest, especially for agricultural crops [3,16–18]. To leverage plant microbiomes to support productivity and resilience both above and below ground [19–21], there is a need to advance foundational knowledge of phyllosphere microbiome diversity and dynamics.

Biofuel crops like miscanthus and switchgrass are selected to have extended growing seasons, to produce ample phyllosphere biomass, and to maintain high productivity when grown on marginal lands that are not optimal for food agriculture [22–25]. In the field, these grasses provide extensive leaf habitat, with a seasonal maximum leaf area index (LAI) of 6.2 for switchgrass, and 10 m^2 leaf surface per m^2 land for miscanthus [22], as compared to a maximum LAI of 3.2 for corn [26]. Upon senescence, the aboveground biomass is harvested for conversion to biofuels and related bioproducts. Improved understanding of the phyllosphere microbiome is expected to advance goals to predict or manage changes in biomass quality in response to abiotic stress like drought [27–31] or biotic stress like foliar pathogens [32–34].

Leveraging the Great Lakes Bioenergy Research Center's Biofuel Cropping System Experiment (BCSE; a randomized block design established at Michigan State's Kellogg Biological Station in 2008), we asked two questions of the bacterial and archaeal communities (henceforth: "microbiomes") inhabiting the leaf surfaces and the associated soils of switchgrass and miscanthus: 1) Are there seasonal patterns of phyllosphere microbiome assembly? If so, are these patterns consistent across fields of the same crop, different crops, and years? 2) To what extent might soil serve as a reservoir of phyllosphere diversity?

Results and Discussion

70 *Sequencing summary and alpha diversity*

71 In total, we sequenced 373 phyllosphere epiphyte (leaf surface) and soil samples across
72 the two growing seasons in 2016 and 2017. The number of sequences per sample after our 97%
73 OTU (operational taxonomic unit) clustering pipeline ranged from 20,647 to 359,553. The
74 percentage of sequences belonging to chloroplasts and mitochondria per sample range
75 between 0.2-99.8%, but 235 of the samples (63%) had fewer than 10% chloroplasts and
76 mitochondria reads. After removing sequences that were attributed to chloroplasts and
77 mitochondria or that had unassigned taxonomic classification, we filtered samples that
78 contained fewer than 1000 reads and rarefied the remaining samples to 1000 reads for
79 comparative analyses. While this number of reads is not sufficient to fully capture soil diversity,
80 it does capture phyllosphere diversity (**Figure 1A**). The majority of the switchgrass and
81 miscanthus phyllosphere communities were exhaustively sequenced, and approached richness
82 asymptotes with their associated soils.

83 As reported for other plants [3,35], switchgrass and miscanthus phyllosphere communities
84 had relatively low richness, with 1480 total taxa observed across both crops and consistently
85 fewer than 150 taxa per time point, though there was modest seasonal variability in richness
86 (**Figure S1**). Cumulative richness increased most between the two earliest time points, and then
87 tapered gradually upward until senescence (**Figure 1B**), showing that the contributions of new
88 taxa to community richness were low but consistent over time.

89

90 *Seasonal microbiome dynamics*

To perform the most complete temporal analyses of phyllosphere microbiome seasonality, we also subsampled the amplicon sequencing dataset to include the maximum number of time points, resulting in inclusion of 51 discrete leaf and soil samples collected over 18 total time points. The overarching patterns in beta diversity were consistent and statistically indistinguishable from those derived from the same dataset to include more reads per sample but fewer time points (Mantel tests all $p < 0.001$; **Table S1, Table S2**, **Figure S2**). For consistency, we report the patterns from 1000 reads per sample in the main text, but for transparency and comparison, we report results from the minimum reads per sample, inclusive of the complete time series, in supporting materials.

There were directional seasonal changes in the structures of switchgrass and miscanthus phyllosphere bacterial and archaeal communities (**Figure 2A**, **Table 1**), and these could be attributed to changes in both soil and leaf properties, as well as to weather (**Table S3**). Over the 2016 season, miscanthus and switchgrass phyllosphere communities were synchronous (changed at the same pace and to the same extent, Procrustes m12= 0.349, R = 0.807, p = 0.021), and community structure became less variable as the growing season progressed (**Figure S3).** Switchgrass 2016 and 2017 leaf communities were highly synchronous, suggesting a predictable, interannual assembly (Procrustes m12= 0.011, R= 0.994, p = 0.008). The switchgrass community structures were overall equivalent between 2016 and 2017, with the exception of the final time points that were collected post-senescence. Together with the species accumulation analysis (**Figure 1B**), these data suggest that these phyllosphere communities are not stochastically assembled, nor are they a linear accumulation over seasonal leaf exposure to whatever taxa are dispersed. The communities follow a directional assembly

113 over the growing season, and the assembly was highly consistent over two years in the
114 switchgrass.

115

116 *Contribution of soil microorganisms to phyllosphere assembly*

117 The major sources of microorganisms to the phyllosphere are soils [2], the vascular tissue
118 of the plant or its seed [36], and the atmosphere or arthropod vectors [3]. As several studies have
119 shown that soil microbes contribute to the phyllosphere microbiome [35,37], we wanted to
120 understand the potential for soil as a reservoir of microorganisms inhabiting switchgrass and
121 miscanthus phyllospheres. We hypothesized that the intersect of shared soil and phyllosphere
122 taxa would be highest early in the season, after the young grasses emerged through the soil.
123 Our deep sequencing effort also provided the opportunity to investigate differences in taxon
124 relative abundances between soil and leaf communities, and to understand what contributions,
125 if any, the soil rare biosphere has for leaf assembly.

126 First, we interrogated the 2016 time series to determine the influence of soil-detected
127 taxa on leaf microbial communities for both crops. As expected, the structures of leaf
128 communities were highly distinct from soils (**Figure 2B**, **Figure S2B**, **Table 1**). Though soil
129 communities also changed seasonally, they experienced less overall change than the
130 phyllosphere (**Table 1**, **Figure 2B**, **Figure S2C**). While fertilization had no impact on phyllosphere
131 communities, it did have small but significant influence on soil communities (**Table 1**). These
132 seasonal and fertilization treatment patterns were reproduced in 2017 for switchgrass (**Table**
133 **1**).

134 To better understand the relationship between soil and phyllosphere communities,
135 including the influence of rare members of the soil, we searched for phyllosphere taxa within
136 the full soil dataset (not subsampled). Approximately 90% of phyllosphere OTUs were present
137 in soil samples, with negligible differences between the two crops and modest variability over
138 time (**Figure 3A**). When considering the relative abundances of taxa, the mean fraction of
139 phyllosphere communities found in soil samples was even higher at 98% and exhibited no clear
140 trend over time (**Figure 3B**). Our results show that the majority of abundant, commonly
141 detected taxa in the phyllosphere are also present in the soil – albeit often at very low
142 abundances (see below) – highlighting a potentially important role of the soil in harboring
143 phyllosphere taxa between plant colonization events.
144 Given the large proportion of phyllosphere taxa present in the soil, we explored the
145 potential role that immigration from the soil may have in shaping phyllosphere community
146 composition and seasonal patterns. On balance, many abundant and persistent phyllosphere
147 taxa were in low abundances in the soil, though there was a positive association between soil
148 and leaf abundances for soil taxa > 1 e04 relative abundance (**Figure 3C**). This result indirectly
149 supports the presence of an ecological filter operating on the phyllosphere that favors some
150 taxa while disfavoring others. To further investigate how ecological filtering may vary over the
151 growing season, we compared observed trends in OTU richness with those predicted by a
152 source-sink null model which simulated demographic stochasticity and random immigration
153 from the soil between subsequent sampling points (see Methods, **Figure 3D-F**). Observed
154 phyllosphere communities were dramatically less rich than null model predictions, again
155 supporting the presence of a strong ecological filter. Such a filter could be due to host plant

156 selection, environmental filtering, competition exclusion among microbial taxa, or a
157 combination of all three. According to this model, the strength of filtering did not trend
158 consistently over the growing season.

159 Finally, other studies have found that soil microbes contribute more to early-season
160 phyllosphere communities [38], and we observed similar patterns: the most abundant soil taxa
161 that were also detected on leaves were more prominent in the early season and then became
162 rare and transient on leaves in the late season (**Figure S4**).

163 We conclude from these results that soil is a major reservoir of leaf microorganisms for
164 these perennial crops and note that deep sequencing was required of the soils to observe many
165 of the prominent leaf taxa. This is in contrast to the studies of other plants that have suggested
166 that the phyllosphere is comprised largely of passively dispersed and stochastically assembled
167 microbes from the atmosphere [39–41]. Notably, our analysis cannot inform directionality or
168 mechanism of dispersal, which could have occurred between soil and leaf via wind, insects, or
169 through grass emergence, etc. While 133 leaf OTUs (9%) observed in the phyllosphere could
170 not be detected in the soil (using the unrarified soil dataset) and may be attributable to non-soil
171 reservoirs, the vast majority of leaf microbes were detectable in local soils and non-neutral
172 assembly patterns suggest both determinism and habitat filtering.

173

174 *Core members of the switchgrass and miscanthus phyllosphere*

175 There was high overlap between switchgrass and miscanthus phyllosphere communities
176 and a trend towards increased intra-crop similarity during senescence (**Figure S5**). There was
177 also a modest influence of host crop in 2016 (**Table 1**). Therefore, we defined a core

178 microbiome for each crop and season (**Dataset 1**). We applied an established macroecological
179 approach [42] to consider both the occupancy and abundance patterns of these taxa (**Figure 4A-**
180 **C)**; abundance-occupancy relationships have been previously explored for microbial
181 communities [43,44] and we utilize it here for ecologically informing a core microbiome.
182 *Occupancy* is an ecological term that considers how consistently a taxon is detected across
183 samples in the dataset, expressed as a proportion of occurrences given the total samples
184 collected (e.g., 1.0 or 100%). Occupancy provides a dataset-aggregated term describing taxon
185 persistence, which can be informative for defining core taxa when datasets include a time
186 series [45].
187 In contrast to the taxa unique to crops and years, which were rare and not persistent,
188 most of the highly abundant and prevalent taxa were shared (**Figure 4A-C**). We first quantified
189 the abundance and occupancy distributions of OTUs, and then identified OTUs that were
190 consistently detected across replicate plots at one sampling time (occupancy of 1) to include in
191 the core. We found that these 44, 51 and 42 core taxa (as highlighted in **Figure 4A-C**) contribute
192 84.4%, 79.5% and 79.4% to the total beta diversity in miscanthus 2016, switchgrass 2016 and
193 2017, respectively (**Figure 4D-F**). While these core taxa were highly abundant and persistent on
194 these crops' leaves, their functions are yet unknown and additional members could also
195 transiently contribute. However, we suggest that the core taxa identified here should be
196 prioritized for follow-up study of functionality and potential plant benefits.
197 Notably, if we had defined the core as those taxa uniquely detected on each crop (as in
198 a Venn diagram analysis, **Figure S6**), we would have instead identified rare and transient taxa
199 (**Figure 4A-C**). Thus, a core analysis based on presence and absence, instead of on abundance

200 and occupancy, would have provided a different, and arguably less ecologically relevant, core
201 for these perennial crops. The approach used here provides a reproducible and conservative
202 option for longitudinal series, and allows for systematic discovery [46,47] of a replicated core over
203 time.

204 The core taxa included several Proteobacteria (*Methylobacterium*, *Sphingomonas*, and
205 *Pseudomonas* spp.) and Bacteroidetes (*Hymenobacter* spp.). The taxonomic affiliations of these
206 core taxa are consistent with the literature for other phyllosphere communities [2,3,18,35,48,49],
207 providing new support for their seasonal importance in the phyllosphere.

208 We then performed a hierarchical clustering analysis of standardized (e.g., z-score)
209 dynamics to explore seasonal trends of core taxa (**Figure 4 G-I, Figure S7**)[50]. This analysis
210 identified several discrete, seasonally-defined groups of core taxa in switchgrass and
211 miscanthus, respectively. Seasonal groups were taxonomically consistent across crops and
212 years (**Figure 4 J-L**). This finding suggests potential for functional redundancy because closely
213 related taxa are hypothesized to have substantial overlap in their functional repertoire [51]. The
214 early-season groups **(Figure S7, Figure 4G-I** red traces**)** included several *Gammaproteobacteria*
215 (**Figure 4J-L**). The late-season groups **(Figure S7, Figure 4G-I** blue traces) was comprised of
216 *Alphaproteobacteria* to *Cytophagia* and *Actinobacteria* and was pronounced in switchgrass
217 (**Figure 4J-L**). The third groups **(Figure S7, Figure 4G-I** gray traces**)** included taxa that peaked in
218 relative abundance mid-season, including *Alphaproteobacteria* and few taxa belonging to *Beta-*
219 and *Gamma-proteobacteria*, *Cytophagia, Sphingobacteria* and *Actinobacteria* (**Figure 4J-L**).

220 Our data suggest a compensatory relationship between members within the
221 Proteobacteria, where members of *Gammaproteobacteria* and *Alphaproteobacteria* replace

222 one another over time (**Figure 5A**). Such community transitions have been observed on the
223 phyllosphere of crops such as sugarcane [37], common beans, soybeans, and canola [38]. A study of
224 endophytic bacteria of prairie grasses, including switchgrass, showed the same trend in
225 abundance of *Gamma*- and *Alphaproteobacteria* [52] suggesting that these phyllosphere taxa are
226 facultative endophytes or are similarly affected by the plant development. The benefits plants
227 may gain from these taxa are well characterized (see review from [53], however it remains
228 unknown what drives the exclusion of *Pseudomonas* and gives rise to *Alphaproteobacteria*
229 (predominantly *Methylobacteria*) in the phyllopshere and endopshere. One possible
230 explanation would be nutrient availability regulated by the plant development which would
231 selectively influence the abundances of these taxa. Delmotte and colleagues [54] hypothesized
232 that *Pseudomonas* specialize on monosaccharides, disaccharides and amino acids, whereas
233 *Sphingomonas* and *Methylobacteria* are generalist scavengers that can subsist on a variety of
234 substrates present at low amounts.

235 Despite similarity in the membership and dynamics of the core microbiota on both crop
236 plants, there were differences in the relative abundances of the same taxa across crops,
237 suggesting some microbiome adaptation to or selectivity by the host plant (**Figure 5B**). There
238 were other core OTUs that had consistent dynamics across both crops, but these examples
239 demonstrate, first, that dynamics can be crop specific, and second, that abiotic filtering of an
240 OTU to a particular crop could be manifested as differences in dynamics in addition to the more
241 extreme scenarios of taxon exclusion or crop specificity that are the hypotheses posed given
242 unique detection on a particular crop. Indeed, because the crop-unique taxa were generally
243 rare and transient (**Figure 4A-C**), the dynamics of core taxa with crop-distinct dynamics may

244 harbor clues as to the competitive landscape and microbially important changes in the host leaf
245 environment across crops.
246
247 *The contributions of abiotic variables, space, time, and crop on phyllosphere assembly*
248 We summarize our analyses of the contributions of crop (host plant), space, time, and
249 abiotic variables to the assembly of the core phyllosphere community in order of least to most
250 important. Spatial distance between the plots had no explanatory value (assessed by distance-
251 decay of beta diversity using a Mantel test with a spatial distance, r: 0.013, p = 0.256). This
252 finding is different from a recent study of annual crops (common beans, canola and soybean)
253 that showed an influenced of sampling location on leaf microbiome structure [38]. Here, among
254 those that variables were significant, crop (switchgrass or miscanthus) had the lowest
255 explanatory value (**Table 1**). However, our work agrees with previous research that has shown a
256 relationship between plant species/genotype and the leaf microbiota of perennial plants such
257 as wild mustard [55], sugar cane [37], and tree species like birch, maple, and pine [56]. Time and
258 measured abiotic factors had highest explanatory value (**Table 1**, **Table S3**). Relatedly, Copeland
259 et al. 2015 showed that stage in plant development can influence leaf microbiome structure in
260 annual crops.
261 To conclude, we investigated the assembly and seasonal dynamics of the phyllosphere
262 and soil microbes of two perennial grasses, switchgrass and miscanthus, and found consistent
263 community trajectories and memberships across growing seasons, suggesting that their key
264 players are predictable and that most of them can be detected in associated soils.
265 Understanding the seasonal patterns of these key taxa could be used to improve biomass

266 production, plant health, or facilitate conversion. As seen in [57], the introduction or control of a
267 few key microbial species can have significant impact on the host plant phenotype. Next steps
268 should be to interrogate core members for functionality and direct interactions with the plant,
269 including investigations of the interactions among core members and with the host crop. This
270 exploration lays the foundation for an approach to biofuel grass production that incorporates
271 an understanding of host-microbe and microbe-microbe interactions.
272
273 Methods
274 *Site description & sampling scheme*
275 Our study system is located within the Great Lakes Bioenergy Research Center (GLBRC)
276 Biofuel Cropping System Experiment (BCSE) in Hickory Corners, Michigan (42°23'41.6" N,
277 85°22'23.1" W). We collected samples from two biofuel crops within the BCSE, switchgrass
278 (*Panicum virgatum* L. cultivar "Cave-in-rock") and miscanthus (*Miscanthus x giganteus)*. Both
279 crops had been continuously grown since 2008, in replicate 30 x 40 m plots arrayed in a
280 randomized complete block design. Within each plot, nitrogen-free (no fertilizer) subplots were
281 maintained in the western-most 3 m of each plot. We sampled replicate plots 1-4 in both the
282 main and the nitrogen free subplots. We collected leaf and bulk soil samples every three weeks
283 across the 2016 growing season, including bare soil in April through senescence in October and
284 November. In total, we collected 152 soil samples (72 switchgrass and 80 miscanthus) and 136
285 leaf samples (64 switchgrass and 72 miscanthus). At each sampling time, leaves were collected
286 and pooled at three flags along a standardized path within each plot. Leaves were removed
287 from the plant stem using ethanol sterilized gloves, then stored in sterile whirl-pak bags until

288 processing. Bulk soil cores (2 x 10 cm) were collected at the same three locations within a plot,
289 sieved through 4 mm mesh, then pooled and stored in whirl-pak bags. All samples were kept
290 on wet ice for transport, then stored at -80 °C.

291 Soil physico-chemical characteristics (pH, lime, P, K, Ca, Mg, organic matter, NO_3-N, NH_4-
292 N, and percent moisture) were measured by the Michigan State University (MSU) Soil and Plant
293 Nutrient Lab (East Lansing, MI, USA, http://www.spnl.msu.edu/) according to their standard
294 protocols. From each plot, 10 switchgrass leaves or 5 miscanthus leaves were processed for
295 leaf dry matter content according to [58]. Dried leaves were ground to a fine powder using a
296 Sampletek 200 vial rotator and iron roll bars (Mavco Industries, Lincoln, NE, USA), then carbon
297 and nitrogen were measured on an elemental analyzer (Costech ECS 4010; Costech Analytical
298 Technologies Inc, Valencia, CA, USA). Weather data was collected from the MSU Weather
299 Station Network, for the Kellogg Biological Station location (https://mawn.geo.msu.edu) for
300 each sampling day, and plant height and soil temperature were measured on a per-plot basis.
301

302 *Nucleic acid extraction & sequencing*

303 Throughout, we use "microbiome" to refer to the bacterial and archaeal members as
304 able to be assessed with 16S rRNA gene sequence analysis. Soil microbial DNA was extracted
305 using a Powersoil microbial DNA kit (MOBio Inc. Carlsbad, California, USA) according to
306 manufacturer's instructions. Phyllosphere epiphytic DNA was extracted from intact leaves using
307 a benzyl chloride liquid:liquid extraction, followed by an isopropanol precipitation [59], using
308 approximately 5 g of leaves (5-10 switchgrass leaves, or a minimum of 2 miscanthus leaves).
309 Metagenomic DNA from both soil and phyllosphere was quantified using a qubit 2.0

310 fluorometer (Invitrogen, Carlsbad, CA, USA), and DNA concentrations were normalized between
311 all samples prior to sequencing. Paired-end amplicon sequencing was completed by the
312 Department of Energy's Joint Genome Institute (JGI) using an Illumina MiSeq sequencer, and
313 using the 16S-V4 (515F-804R) primer set [60], according to the JGI's standard operating protocols,
314 and incorporating chloroplast- and mitochondria-blocking peptide nucleic acids to prevent co-
315 amplification of plastid 16S rRNA gene as described in [61].
316 .
317
318 *Sequence quality control and defining operational taxonomic units*
319 BBDuk (v 37.96) was used to remove contaminants and trim adaptor sequences from
320 reads. Reads containing 1 or more 'N' bases, having an average quality score of less than ten or
321 less than 51 bases were removed. Common contaminants were removed with BBMap (v 37.96).
322 Primers were trimmed using cutadapt (v1.17). Reads were merged, dereplicated, clustered into
323 97% identity with usearch (v10.0.240), and classified against version 123 of the Silva Database
324 [62] using sintax [63]. All reads classified as mitochondria, chloroplast or unclassified were removed
325 before the analysis. Additionally, reads from 4371 OTUs assigned only to the domain level were
326 extracted and reclassified using SINA online aligner (https://www.arb-silva.de/aligner/) [62]. 696
327 unclassified reads subsequently were confirmed to be Bacteria could then be classified to more
328 resolved taxonomic levels. Remaining reads were BLASTed against the entire NCBI nucleotide
329 database and specifically against the switchgrass genome to check for non-specific binding, but
330 no hits could be found.
331

332 *Alpha and beta diversity*

333 For alpha and beta diversity analyses, we performed analyses to datasets subsampled to
334 the minimum observed quality-filtered reads per sample (141), as well as to 1000 reads per
335 sample. We did this to enable comparison of the most complete time series to the most
336 complete comparative view of diversity. We report richness as total number of OTUs clustered
337 at 97% sequence identity. We used the protest function in the vegan package in R [64] to test for
338 synchrony in patterns across crops and years. To calculate beta dispersion, we used the
339 betadisper function in the vegan package in R [64], which is a multivariate analogue of Levene's
340 test for homogeneity of variances. PERMANOVA was used to test hypothesis of beta diversity
341 using adonis function in the vegan package in R [64].

342

343 *Source-sink models and contributions of soil taxa to leaf communities*

344 Given that virtually all phyllosphere taxa were present in the soil, we evaluated the degree to
345 which observed seasonal patterns in phyllosphere community composition could be explained
346 with a null model. The null model assumed functional equivalence among taxa and random
347 source-sink dynamics from the soil. For each crop, we simulated community dynamics between
348 each pair of sequential samples. This involved: (1) calculating the total number of 0.1 %
349 incremental increases/decreases in OTU relative abundances observed between the two
350 sampling points; (2) randomly and iteratively selecting OTUs, weighting their probability of
351 selection by their relative abundances, to increase or decrease by 0.1 % increments of relative
352 abundance until reaching the total number of observed increases/decreases for the sample
353 pair; (3) counting the number of immigrant OTUs which appeared only in the second sample of

354 the pair; (4) randomly selecting OTUs in the simulated community to decrease by 0.1 %
355 increments until the total decrease equaled the observed number of arriving OTUs multiplied
356 by their median initial abundance (0.1 %); and then (5) randomly selecting, again weighting
357 their probability of selection by their relative abundance, the predicted number of immigrant
358 OTUs from the soil community, such that the final simulated community abundance was equal
359 to 1000 sequences. The source soil community was generated by pooling all soil samples from
360 both years. We used this process to simulate demographic stochasticity. In the model, it was
361 assumed that 0.1 % incremental changes in relative abundance realistically reflects
362 phyllosphere population dynamics, and that an immigration event results in the initial relative
363 abundance of an OTU at 0.1%. Importantly, even if these assumptions are imprecise, the
364 simulation provides a consistent baseline of community composition against which to compare
365 observations over the growing season.
366
367 *Core taxa selection*
368 To infer the core phyllosphere taxa and prioritize them for further inquiry, we calculated the
369 abundance-occupancy distributions of taxa, as established in macroecology (e.g. Shade et al.
370 2018). For each OTU, we calculated occupancy and mean relative abundance at each time point
371 by crop and year. Only OTUs with occupancy of 100% (found in all samples at a particular time
372 point) were prioritized as core members. Using this conservative threshold for occupancy, we
373 included all OTUs that had strong temporal signatures; these taxa also were in high abundance
374 and were persistent as indicated by their abundance-occupancy distributions. These core taxa

375 also represent potentially important players in plant development, as they were detected at
376 least at one time point in all sampled fields.
377 We quantified the explanatory value of the core members to community temporal
378 dynamics using a previously published method of partitioning community dissimilarity [65]:

379 $$C = \frac{BC_{core}}{BC_{all}}$$

380 Where *C* is the relative contribution of community Bray Curtis (*BC*) dissimilarity
381 attributed to the core OTUs.
382
383 *Hierarchical clustering*
384 To understand the seasonal abundance patterns of the core taxa we performed
385 hierarchical clustering. We used a z-scored relative abundance matrix subset to contain only
386 core taxa to generate a w complete linkage distance matrix using the R function hclust() [50].
387 Groups of core taxa with similar dynamics were defined from the dendrogram using the
388 function cutree() in R with number of desired groups (k=) to be close to the number of sampling
389 time points; 8 for miscanthus 2016, 5 for switchgrass 2016 and 7 for switchgrass 2017.
390
391 *Availability of data, workflows, and material*
392 The datasets generated and/or analyzed during the current study are available in the
393 Joint Genomes Institute, Integrated Microbial Genomes repository with JGI Projects designated
394 by year and sample type (Project ID 1139694, 1139696 for 2016 season phyllosphere and soil,
395 and 1191516 and 1191517 for 2017 season phyllosphere and soil sequences, respectively). Our

396 sequence analyses and statistical workflows are available at

397 https://github.com/ShadeLab/PAPER_GradySorensenStopnisek_InPrep

398

399 Competing interests

400 The authors declare that they have no competing interests.

401

402 Authors' contributions

403 AS designed the study. AS, KLG, JS, and NS conducted field work. KLG executed lab work. JS,

404 NS, JG, and AS analyzed the data. All authors discussed and revised the manuscript.

405

406 Acknowledgements

407 We thank SH Lee, M Sleda, S Wu and M Nunez for technical assistance in the field and

408 laboratory. This material is based upon work supported by the Great Lakes Bioenergy Research

409 Center, U.S. Department of Energy, Office of Science, Office of Biological and Environmental

410 Research under Award Numbers DE-SC0018409 and DE-FC02-07ER64494. The work conducted

411 by the U.S. Department of Energy Joint Genome Institute, a DOE Office of Science User Facility,

412 is supported under Contract No. DE-AC02-05CH11231. This work was supported in part by

413 Michigan State University through computational resources provided by the Institute for Cyber-

414 Enabled Research. NS acknowledges support from the Michigan State Plant Resilience Institute.

415

416

417

418 Figure Legends

419 **Figure 1. Sequencing effort and alpha diversity for switchgrass and miscanthus phyllosphere**
420 **and soils.** Operational taxonomic units (OTUs) were defined at 97% sequence identity of 16S
421 rRNA gene amplicons. (A) Rarefaction curves of quality-controlled reads. The vertical line is the
422 maximum number of sequences observed in a sample, and the horizontal line is the richness of
423 that sample. (B) Phyllosphere richness accumulation over time, using a dataset subsampled to
424 1000 sequences per sample.

425

426 **Figure 2. Seasonal patterns in the structures of bacterial and archaeal communities**
427 **inhabiting the phyllosphere and associated soils of the biofuel feedstocks switchgrass and**
428 **miscanthus.** (A) Principal coordinates analysis (PCoA) of switchgrass and miscanthus
429 phyllosphere communities (Bray-Curtis dissimilarity), error bars show 1 deviation around the
430 centroid (n = 1 to 8 replicate plots/time point). (B) PCoA of the phyllosphere communities
431 relative to the soil. For both A and B, subsampling depth was 1000 reads per sample and
432 environmental vectors were fitted when $r^2 > 0.4$ and $p < 0.05$.

433

434 **Figure 3. The majority of phyllosphere taxa were also present in the soil.** (**A**) Circles represent
435 the mean number of OTUs found in up to eight replicate phyllosphere samples, subsampled to
436 1000 sequences, for each crop at each time point. An OTU was considered present in the soil if
437 it occurred at any abundance in any of the 202 unrarefied soil samples over two years. **(B)** The
438 fractions of the phyllosphere communities present in the soil were even greater when
439 considering the relative abundances of taxa; each circle represents the mean total relative

440 abundance of leaf taxa present in the soil in up to four replicate phyllosphere samples. **(C)** The
441 relative abundances of taxa in pooled phyllosphere samples and pooled soil samples were
442 positively correlated among taxa that were present at greater than 0.01% total abundance in
443 the soil. Each black circle represents an OTU present in both phyllosphere and soil
444 communities; a LOESS smoothing function is shown as a red line. Core members are shown as
445 large green circles. (**D-F**) Source-sink models of phyllosphere community assembly from soils.
446 Violin plots show the numbers of observed taxa in the phyllosphere were consistently lower
447 than the richness values predicted by model simulations. The model assumed random increases
448 and decreases in taxon abundances between time points and random immigration from the soil
449 community (see Methods). Each circle represents a single phyllosphere sample.
450
451 **Figure 4**. **Selection and dynamics of core phyllosphere members.** Abundance-occupancy of
452 leaf taxa for **(A)** miscanthus 2016, **(B)** switchgrass 2016, and **(C)** switchgrass 2017, and their
453 inclusion in their respective cores. Each point is an OTU. Abundance-occupancy distributions
454 were calculated at each time point, and taxa that had 100% occupancy at any time point (e.g.,
455 were detected in all replicate plots at one sampling date) were included in the core (green).
456 Non-core taxa that were detected in both crops (white/open circles), and crop-specific taxa
457 (grey) are also indicated. (**D-F**) Contributions of the core taxa to changes in beta diversity over
458 time. (**G-I**) Patterns of core taxa that share similar temporal changes, as determined by
459 hierarchical clustering of standardized dynamics. Colors correspond to the dendrograms in
460 **Figure S7**. (**J-L**) Patterns of core taxa summed by relative abundances within bacterial class.
461 "c:" is class and "p:" is phylum.

462

463 **Figure 5. Compensatory patterns of Protobacteria classes over crops and season in the**

464 **phyllosphere of switchgrass and miscanthus**. Proteobacteria OTUs contributed 35.2% of the

465 total taxa detected in the phyllosphere and contributed 116,760 total reads (34.1% of the leaf

466 reads). **(A)** Changes in the relative contributions of all 521 leaf-detected Proteobacteria OTUs by

467 class, over time. **(B-D)** Vignettes showing different dynamics of Proteobacteria OTUs that were

468 detected within the phyllosphere core microbiome, over time and across crops. Class is "c:"

469 and genus is "g:".

470

471

Table

Table 1. Permuted multivariate analysis of variance (PERMANOVA) tables for all hypothesis tests for differences in community structure (beta diversity).

478 Supporting Figures

479 **Figure S1. Seasonal patterns in the number of observed phyllosphere taxa (richness).**

480 Operational taxonomic units (OTUs) were defined at 97% amplicon sequence identity. Richness

481 is provided at subsampling depths of 1000 reads (top) and 141 reads (bottom).

482

483 **Figure S2. Seasonal patterns in the structures of bacterial and archaeal communities**

484 **inhabiting the phyllosphere and associated soils of the biofuel feedstocks switchgrass and**

485 **miscanthus.** (A) Principal coordinates analysis (PCoA) of switchgrass and miscanthus

486 phyllosphere communities (Bray-Curtis dissimilarity), error bars show 1 deviation around the

487 centroid (n = 3 to 8 replicate plots/time point). Subsampling depth was 141 reads per sample

488 and environmental vectors are fitted when $r^2 > 0.4$ and $p < 0.05$. **(B)** PCoA of the phyllosphere

489 communities relative to the soil, subsampled to 141 sequences per sample. **(C)** PCoA of the soil

490 communities associated with miscanthus and switchgrass, subsampled to 19,967 sequences per

491 sample.

492

493 **Figure S3. Phyllosphere communities become less variable over time**. Distance to median was

494 calculated by analysis of beta-dispersion. Variability in phyllosphere microbiome structure over

495 time miscanthus 2016, switchgrass 2016, and switchgrass 2017 field seasons. Betadispersion

496 was calculated from data series subsampled to 1000 reads (top) and 141 reads (bottom).

497

498 **Figure S4**. **Decreases in the contributions of soil-dominating taxa to the phyllosphere**

499 **microbiome over time**. Heatmaps represent the 50 top-ranked OTUs from the soil that were

500 also detected in the phyllosphere. The cell colors are the z-scored relative abundances of the
501 OTUs in the phyllosphere. The ranking is from top to bottom (e.g., the most abundant soil-
502 dominant taxon that was also detected in the phyllosphere is represented by the top row in the
503 heatmap). The left bar shows the classification the taxon as either a core member (green) or
504 not (pink). **(A)** Miscanthus 2016; **(B)** switchgrass 2016; **(C)** switchgrass 2017.
505
506 **Figure S5. Intra-crop similarity in leaf communities over time in 2016**. We show changes in
507 Bray-Curtis dissimilarities between switchgrass and miscanthus phyllosphere microbiomes per
508 time point, inclusive of the maximum number of replicated blocks (up to 8) per time point. **(A)**
509 "Full" time series, subsampled to 141 reads per sample. **(B)** Time series subsampled to 1000
510 reads per sample.
511
512 **Figure S6. Venn diagram of taxa shared across the switchgrass and miscanthus phyllosphere,**
513 in 2016 and 2017. Data were rarefied to 1000 reads per sample.
514
515 **Figure S7. Hierarchical clustering of standardized (z-scored) dynamics of core phyllosphere**
516 **taxa on the phyllosphere of miscanthus 2016 (A), switchgrass 2016 (B) and switchgrass 2017**
517 **(C).** Seasonally discrete clusters coincide with plant phenology, including groups that achieved
518 highest relative abundance during early (red), mid (gray) and late (blue) plant growth. Clusters
519 are labeled in order of temporal occurrence in **Figure 4G-I**. Circles on the dendrogram tips are
520 color coded by OTU taxonomic classification and labeled with the OTU ID.
521

522
523 Supporting Tables

524 **Table S1**. **Sequencing summary of phyllosphere microbial communities characterized in this**

525 **study**, categorized by crop and year.

526

527 **Table S2**. **Comparison of overarching patterns of beta diversity across the same dataset**

528 **rarefied to different sequencing depths**. We compared all pairs of 141, 500, 1000, 5000, or

529 10000 reads per sample. All Mantel tests were significant at $p < 0.001$ on 1000 permutations.

530

531 **Table S3**. Fitted environmental variables that explain changes in microbiome community

532 structure. Values in which EnvFit $R^2 > 0.40$ were plotted as vectors in **Figure 2**.

533

534 Datasets

535 **Dataset 1.** Operational taxonomic unit identifiers and representative 16S rRNA gene amplicon

536 sequences of the core switchgrass and miscanthus phyllosphere microbiota.

537

538

539 **References**

540 1. Peñuelas, J. & Terradas, J. The foliar microbiome. *Trends Plant Sci.* **19**, 278–280 (2014).

541 2. Lindow, S. E. & Brandl, M. T. Microbiology of the phyllosphere. *Appl. Environ. Microbiol.*
542 **69**, 1875–1883 (2003).

543 3. Vorholt, J. A. Microbial life in the phyllosphere. *Nat. Rev. Microbiol.* **10**, 828–840 (2012).

544 4. Foley, J. A. *et al.* Solutions for a cultivated planet. *Nature* **478**, 337–342 (2011).

545 5. Hamilton, C. E., Gundel, P. E., Helander, M. & Saikkonen, K. Endophytic mediation of
546 reactive oxygen species and antioxidant activity in plants: a review. *Fungal Divers.* **54**, 1–
547 10 (2012).

548 6. Lindow, S. E. & Leveau, J. H. J. Phyllosphere microbiology. *Curr. Opin. Biotechnol.* **13**,
549 238–243 (2002).

550 7. Redman, R. S., Sheehan, K. B., Stout, R. G., Rodriguez, R. J. & Henson, J. M.
551 Thermotolerance generated by plant/fungal symbiosis. *Science* **298**, 1581 (2002).

552 8. Canto, A. & Herrera, C. M. Micro-organisms behind the pollination scenes: Microbial
553 imprint on floral nectar sugar variation in a tropical plant community. *Ann. Bot.* **110**,
554 1173–1183 (2012).

555 9. Doty, S. L. *et al.* Diazotrophic endophytes of native black cottonwood and willow.
556 *Symbiosis* **47**, 23–33 (2009).

557 10. Taghavi, S. *et al.* Genome survey and characterization of endophytic bacteria exhibiting a
558 beneficial effect on growth and development of poplar trees. *Appl. Environ. Microbiol.*
559 **75**, 748–757 (2009).

560 11. Lee, D. W., Hong, J. S., Kim, S. H., Kim, J. W. & Kim, B. S. First Report of Pseudomonas

561 lurida Causing Bacterial Leaf Spot on Miscanthus sinensis. *J. Phytopathol.* **162**, 195–200
562 (2014).
563 12. Wagner, M. R. *et al.* Natural soil microbes alter flowerig phenology and the intensity of
564 selection on flowering time in a wild *Arabidopsis* relative`. *Ecol. Lett.* **17**, 717–726 (2014).
565 13. Iguchi, M., Yamanaka, S. & Budhiono, A. Bacterial cellulose - a masterpiece of nature's
566 arts. *J. Mater. Sci.* **35**, 261–270 (2000).
567 14. Galbally, I. E. & Kirstine, W. The production of methanol by flowering plants and the
568 global cycle of methanol. *J. Atmos. Chem.* **43**, 195–229 (2002).
569 15. Fürnkranz, M. *et al.* Nitrogen fixation by phyllosphere bacteria associated with higher
570 plants and their colonizing epiphytes of a tropical lowland rainforest of Costa Rica. *ISME*
571 *J.* **2**, 561–570 (2008).
572 16. Weyens, N., van der Lelie, D., Taghavi, S., Newman, L. & Vangronsveld, J. Exploiting plant-
573 microbe partnerships to improve biomass production and remediation. *Trends in*
574 *Biotechnology* **27**, 591–598 (2009).
575 17. Hacquard, S. & Schadt, C. W. Towards a holistic understanding of the beneficial
576 interactions across the *Populus* microbiome. *New Phytologist* **205**, 1424–1430 (2015).
577 18. Kinkel, L. L. Microbial Population Dynamics on Leaves. *Annu. Rev. Phytopathol.* **35**, 327–
578 347 (1997).
579 19. Lebeis, S. L. The potential for give and take in plant-microbiome relationships. *Front.*
580 *Plant Sci.* **5**, 1–6 (2014).
581 20. Vandenkoornhuyse, P., Quaiser, A., Duhamel, M., Le Van, A. & Dufresne, A. The
582 importance of the microbiome of the plant holobiont. *New Phytol.* **206**, 1196–1206

583 (2015).

584 21. Turner, T. R., James, E. K. & Poole, P. The plant microbiome. *Genome Biol.* **14**, (2013).

585 22. Heaton, E. A., Dohleman, F. G. & Long, S. P. Meeting US biofuel goals with less land: The

586 potential of Miscanthus. *Glob. Chang. Biol.* **14**, 2000–2014 (2008).

587 23. Tornqvist, C. E. *et al.* Transcriptional Analysis of Flowering Time in Switchgrass. *Bioenergy*

588 *Res.* **10**, 700–713 (2017).

589 24. Robertson, G. P. *et al.* Cellulosic biofuel contributions to a sustainable energy future:

590 Choices and outcomes. *Science.* **356**, 1-9 (2017).

591 25. Stoof, C. R. *et al.* Untapped Potential: Opportunities and Challenges for Sustainable

592 Bioenergy Production from Marginal Lands in the Northeast USA. *BioEnergy Res.* **8**, 482–

593 501 (2015).

594 26. Johnson, D. R. & Tanner, J. W. Comparisons of Corn (*Zea mays* L .) Inbreds and Hybrids

595 Grown at Equal Leaf Area Index , Light Penetration , and Population is generally accepted

596 that corn hybrids (*Zea raays* I T L .) are superior to inbred lines in terms of overall size

597 and yield . At a. 482–485 (1972).

598 27. Wang, B., Seiler, J. R. & Mei, C. A microbial endophyte enhanced growth of switchgrass

599 under two drought cycles improving leaf level physiology and leaf development. *Environ.*

600 *Exp. Bot.* **122**, 100–108 (2016).

601 28. Ong, R. G. *et al.* Inhibition of microbial biofuel production in drought-stressed

602 switchgrass hydrolysate. *Biotechnol. Biofuels* **9**, 1–14 (2016).

603 29. Emerson, R. *et al.* Drought effects on composition and yield for corn stover, mixed

604 grasses, and Miscanthus as bioenergy feedstocks. *Biofuels* **5**, 275–291 (2014).

605 30. Fitzpatrick, C. R. *et al.* Assembly and ecological function of the root microbiome across
606 angiosperm plant species. *Proc. Natl. Acad. Sci.* 201717617 (2018).
607 31. Santos-Medellín, C., Edwards, J., Liechty, Z., Nguyen, B. & Sundaresan, V. Drought Stress
608 Results in a Compartment-Specific Restructuring of. *MBio* **8**, 1–15 (2017).
609 32. Cox, C. M., Bockus, W. W., Holt, R. D., Fang, L. & Garrett, K. A. Spatial connectedness of
610 plant species: Potential links for apparent competition via plant diseases. *Plant Pathol.*
611 **62**, 1195–1204 (2013).
612 33. Alexander, H. M., Bruns, E., Schebor, H. & Malmstrom, C. M. Crop-associated virus
613 infection in a native perennial grass: reduction in plant fitness and dynamic patterns of
614 virus detection. *J. Ecol.* **105**, 1021–1031 (2017).
615 34. Sattler, S. E. & Funnell-Harris, D. L. Modifying lignin to improve bioenergy feedstocks:
616 strengthening the barrier against pathogens? *Front. Plant Sci.* **4**, 1–8 (2013).
617 35. Bodenhausen, N., Horton, M. W. & Bergelson, J. Bacterial Communities Associated with
618 the Leaves and the Roots of *Arabidopsis thaliana*. *PLoS One* **8**, (2013).
619 36. Barret, M. *et al.* Emergence shapes the structure of the seed microbiota. *Appl. Environ.*
620 *Microbiol.* **81**, 1257–1266 (2015).
621 37. Hamonts, K. *et al.* Field study reveals core plant microbiota and relative importance of
622 their drivers. *Environ. Microbiol.* **20**, 124–140 (2018).
623 38. Copeland, J. K., Yuan, L., Layeghifard, M., Wang, P. W. & Guttman, D. S. Seasonal
624 Community Succession of the Phyllosphere Microbiome. *Mol. Plant-Microbe Interact.* **28**,
625 274–285 (2015).
626 39. Ottesen, A. R. *et al.* Using a Control to Better Understand Phyllosphere Microbiota. *PLoS*

627 *One* **11**, 1-16 (2016).

628 40. Maignien, L., DeForce, E. A., Chafee, M. E., Murat Eren, A. & Simmons, S. L. Ecological
629 succession and stochastic variation in the assembly of *Arabidopsis thaliana* phyllosphere
630 communities. *MBio* **5**, (2014).

631 41. Vokou, D. *et al.* Exploring biodiversity in the bacterial community of the mediterranean
632 phyllosphere and its relationship with airborne bacteria. *Microb. Ecol.* **64**, 714–724
633 (2012).

634 42. Gaston, K. J. *et al.* Abundance - occupancy relationships. *J. Appl. Ecol.* **37**, 39–59 (2000).

635 43. Shade, A. *et al.* Macroecology to unite all life, large and small. *Trends Ecol. Evol.* (2018).

636 44. Burns, A. R. *et al.* Contribution of neutral processes to the assembly of gut microbial
637 communities in the zebrafish over host development. *ISME J.* **10**, 655–664 (2016).

638 45. Shade, A. & Handelsman, J. Beyond the Venn diagram: The hunt for a core microbiome.
639 *Environ. Microbiol.* **14**, 4–12 (2012).

640 46. Astudillo-García, C. *et al.* Evaluating the core microbiota in complex communities: A
641 systematic investigation. *Environ. Microbiol.* **19**, 1450–1462 (2017).

642 47. Shade, A. *et al.* Culturing captures members of the soil rare biosphere. *Environmental*
643 *Microbiology* **14**, 2247–2252 (2012).

644 48. Knief, C., Ramette, A., Frances, L., Alonso-Blanco, C. & Vorholt, J. A. Site and plant species
645 are important determinants of the *Methylobacterium* community composition in the
646 plant phyllosphere. *ISME J.* **4**, 719–728 (2010).

647 49. Rastogi, G., Coaker, G. L. & Leveau, J. H. J. J. New insights into the structure and function
648 of phyllosphere microbiota through high-throughput molecular approaches. *FEMS*

649 *Microbiol. Lett.* **348**, 1–10 (2013).

650 50. R Core Team. R: A language and environment for statistical computing. R Foundation for
651 Statistical Computing, Vienna, Austria. https://www.R-project.org/.(2018).

652 51. Martiny, J. B. H., Jones, S. E., Lennon, J. T. & Martiny, A. C. Microbiomes in light of traits:
653 A phylogenetic perspective. *Science (80).* **350**, (2015).

654 52. Ding, T. & Melcher, U. Influences of plant species, season and location on leaf endophytic
655 bacterial communities of non-cultivated plants. *PLoS One* **11**, 1–13 (2016).

656 53. Bringel, F. & Couée, I. Pivotal roles of phyllosphere microorganisms at the interface
657 between plant functioning and atmospheric trace gas dynamics. *Front. Microbiol.* **6**,
658 (2015).

659 54. Delmotte, N. *et al.* Community proteogenomics reveals insights into the physiology of
660 phyllosphere bacteria. *Proc. Natl. Acad. Sci.* **106**, 16428–16433 (2009).

661 55. Wagner, M. R. *et al.* Host genotype and age shape the leaf and root microbiomes of a
662 wild perennial plant. *Nat. Commun.* **7**, 12151 (2016).

663 56. Laforest-Lapointe, I., Messier, C. & Kembel, S. W. Tree phyllosphere bacterial
664 communities: exploring the magnitude of intra- and inter-individual variation among host
665 species. *PeerJ* **4**, e2367 (2016).

666 57. Agler, M. T. *et al.* Microbial Hub Taxa Link Host and Abiotic Factors to Plant Microbiome
667 Variation. *PLoS Biol.* **14**, 1–31 (2016).

668 58. Cornelissen, J. H. C. *et al.* A handbook of protocols for standardised and easy
669 measurement of plant functional traits worldwide. *Aust. J. Bot.* **51**, 335–380 (2003).

670 59. Suda, W., Oto, M., Amachi, S., Shinoyama, H. & Shishido, M. A Direct Method to Isolate

671 DNA from Phyllosphere Microbial Communities without Disrupting Leaf Tissues.
672 *Microbes Environ.* **23**, 248–252 (2008).
673 60. Caporaso, J. G. *et al.* Moving pictures of the human microbiome. *Genome Biol.* **12**,
674 (2011).
675 61. Lundberg, D. S., Yourstone, S., Mieczkowski, P., Jones, C. D. & Dangl, J. L. Practical
676 innovations for high-throughput amplicon sequencing. *Nat. Methods* **10**, 999–1002
677 (2013).
678 62. Quast, C. *et al.* The SILVA ribosomal RNA gene database project: Improved data
679 processing and web-based tools. *Nucleic Acids Res.* **41**, (2013).
680 63. Edgar, R. C. SINTAX: a simple non-Bayesian taxonomy classifier for 16S and ITS
681 sequences. *Preprint at* doi:10.1101/074161 (2016).
682 64. Oksanen, J. *et al.* vegan: Community Ecology Package. R Package version 2.5-2. (2018).
683 65. Shade, A. *et al.* Conditionally rare taxa disproportionately contribute to temporal
684 changes in microbial diversity. *MBio* **5**, 1–9 (2014).
685

Figure 1

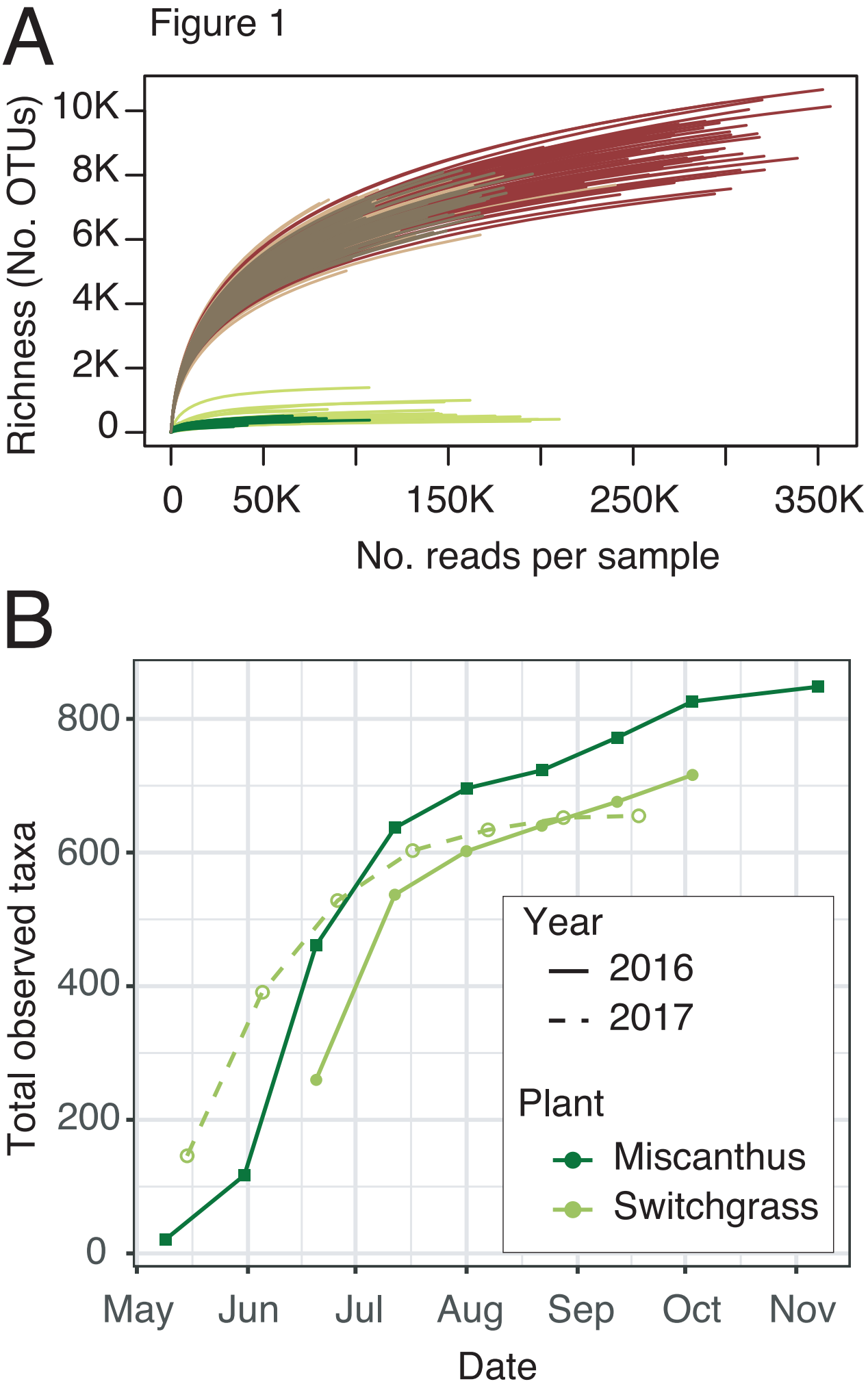
A
Richness (No. OTUs)
10K
8K
6K
4K
2K
0
0
50K
150K
250K
350K
No. reads per sample
B
Total observed taxa
800
600
400
200
0
May
Jun
Jul
Aug
Sep
Oct
Nov
Date
Year
2016
2017
Plant
Miscanthus
Switchgrass

Figure 2

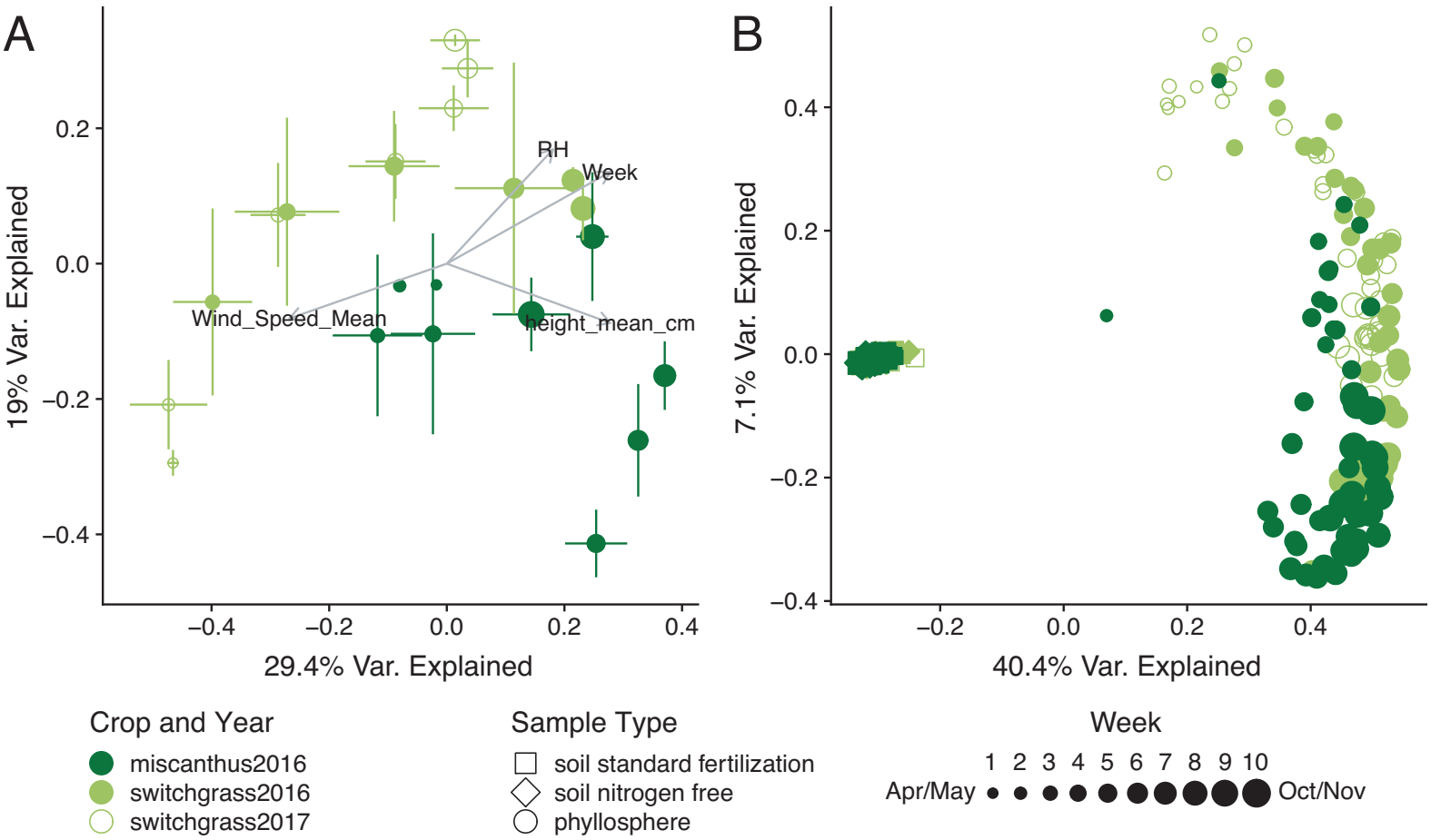
A
B
RH
Week
Wind_Speed_Mean
height_mean_cm
19% Var. Explained
29.4% Var. Explained
7.1% Var. Explained
40.4% Var. Explained
0.2
0.0
−0.2
−0.4
0.4
Crop and Year
miscanthus2016
switchgrass2016
switchgrass2017
Sample Type
soil standard fertilization
soil nitrogen free
phyllosphere
Week
1 2 3 4 5 6 7 8 9 10
Apr/May
Oct/Nov

Figure 3

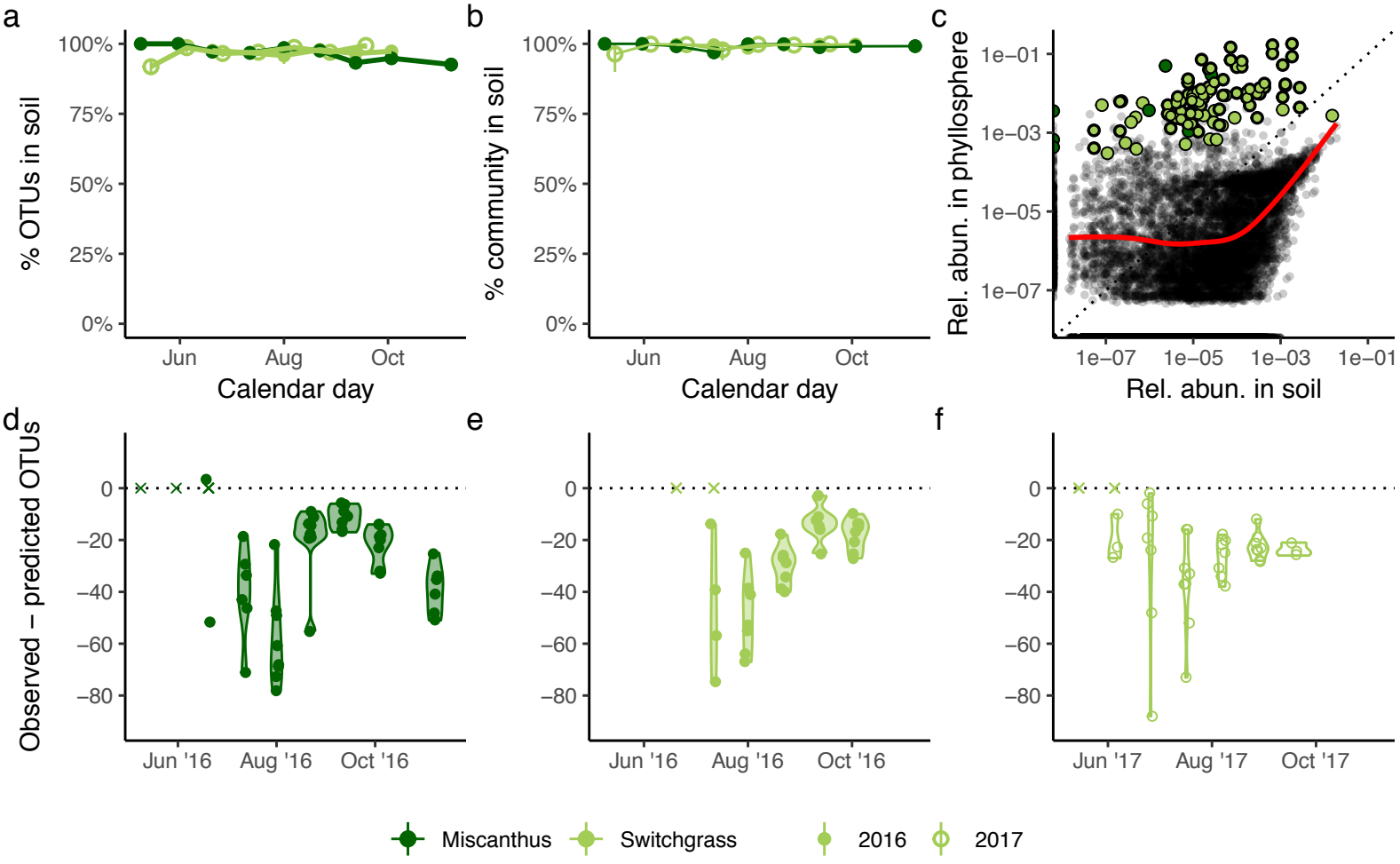
a
b
c
d
e
f
% OTUs in soil
% community in soil
Rel. abun. in phyllosphere
Rel. abun. in soil
Calendar day
100%
75%
50%
25%
0%
Jun
Aug
Oct
1e−01
1e−03
1e−05
1e−07
Observed − predicted OTUs
0
−20
−40
−60
−80
Jun '16
Aug '16
Oct '16
Jun '17
Aug '17
Oct '17
Miscanthus
Switchgrass
2016
2017

Figure 4

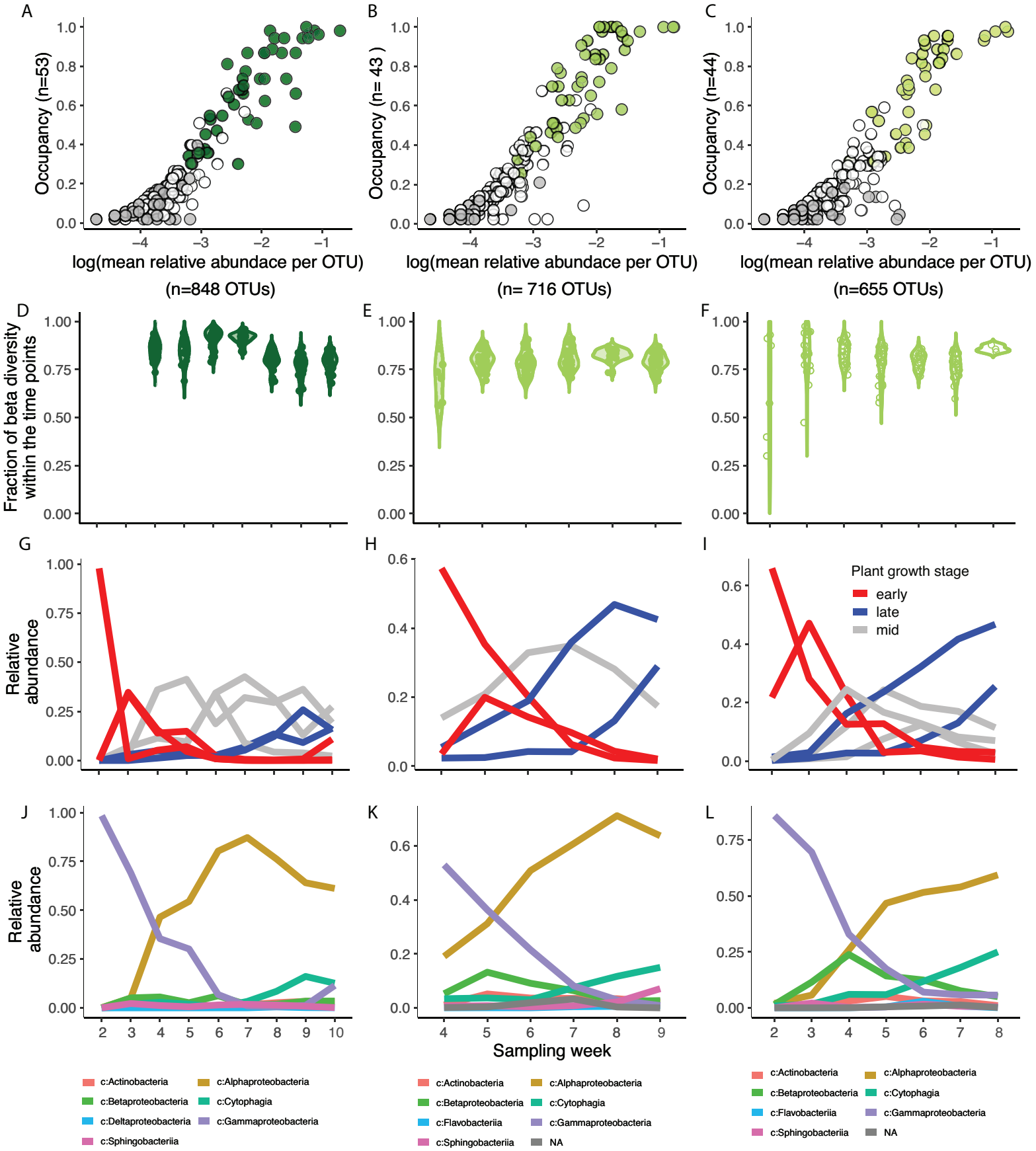
A
B
C
Occupancy (n=53)
Occupancy (n= 43)
Occupancy (n=44)
log(mean relative abundace per OTU)
(n=848 OTUs)
(n= 716 OTUs)
(n=655 OTUs)
D
E
F
Fraction of beta diversity within the time points
G
H
I
Relative abundance
Plant growth stage
early
late
mid
J
K
L
Relative abundance
Sampling week
c:Actinobacteria
c:Alphaproteobacteria
c:Betaproteobacteria
c:Cytophagia
c:Deltaproteobacteria
c:Gammaproteobacteria
c:Sphingobacteriia
c:Flavobacteriia
NA

Figure 5

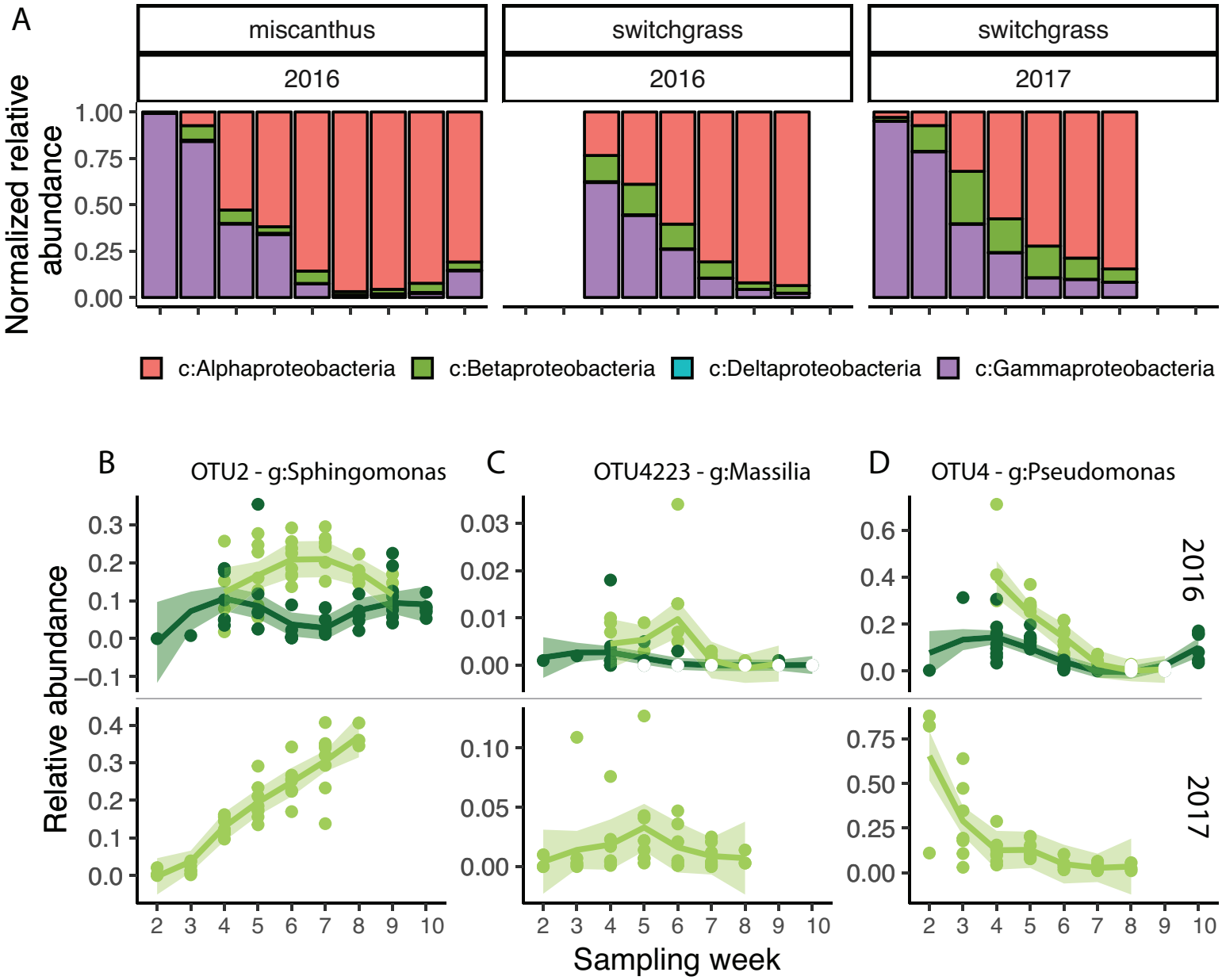
A
miscanthus
2016
switchgrass
2016
switchgrass
2017
Normalized relative abundance
1.00
0.75
0.50
0.25
0.00
c:Alphaproteobacteria
c:Betaproteobacteria
c:Deltaproteobacteria
c:Gammaproteobacteria
B
OTU2 - g:Sphingomonas
C
OTU4223 - g:Massilia
D
OTU4 - g:Pseudomonas
Relative abundance
2016
2017
Sampling week

Table 1. Permuted multivariate analysis of variance (PERMANOVA) tables for all hypothesis tests for differences in community structure (beta diversity).

Dataset	Variable Tested	Degrees of Freedom	PseudoF	R squared	p-value
2016 All	Microbiome habitat (soil v. leaf)	1	166.09	0.415	0.001
2017 All	Microbiome habitat (soil v. leaf)	1	74.66	0.418	0.001
2016 Phyllosphere	Time	1	21.02	0.183	0.001
2016 Soil	Time	1	7.31	0.050	0.001
2017 Phyllosphere	Time	1	29.09	0.409	0.001
2017 Soil	Time	1	3.05	0.048	0.001
2016 Phyllosphere	Crop	1	14.50	0.134	0.001
2016 Soil	Crop	1	6.76	0.047	0.001
2016 Phyllosphere	Fertilization status	1	0.40	0.004	0.95
2016 Soil	Fertilization status	1	4.77	0.033	0.001
2017 Phyllosphere	Fertilization status	1	0.87	0.020	0.438
2017 Soil	Fertilization status	1	3.41	0.054	0.001

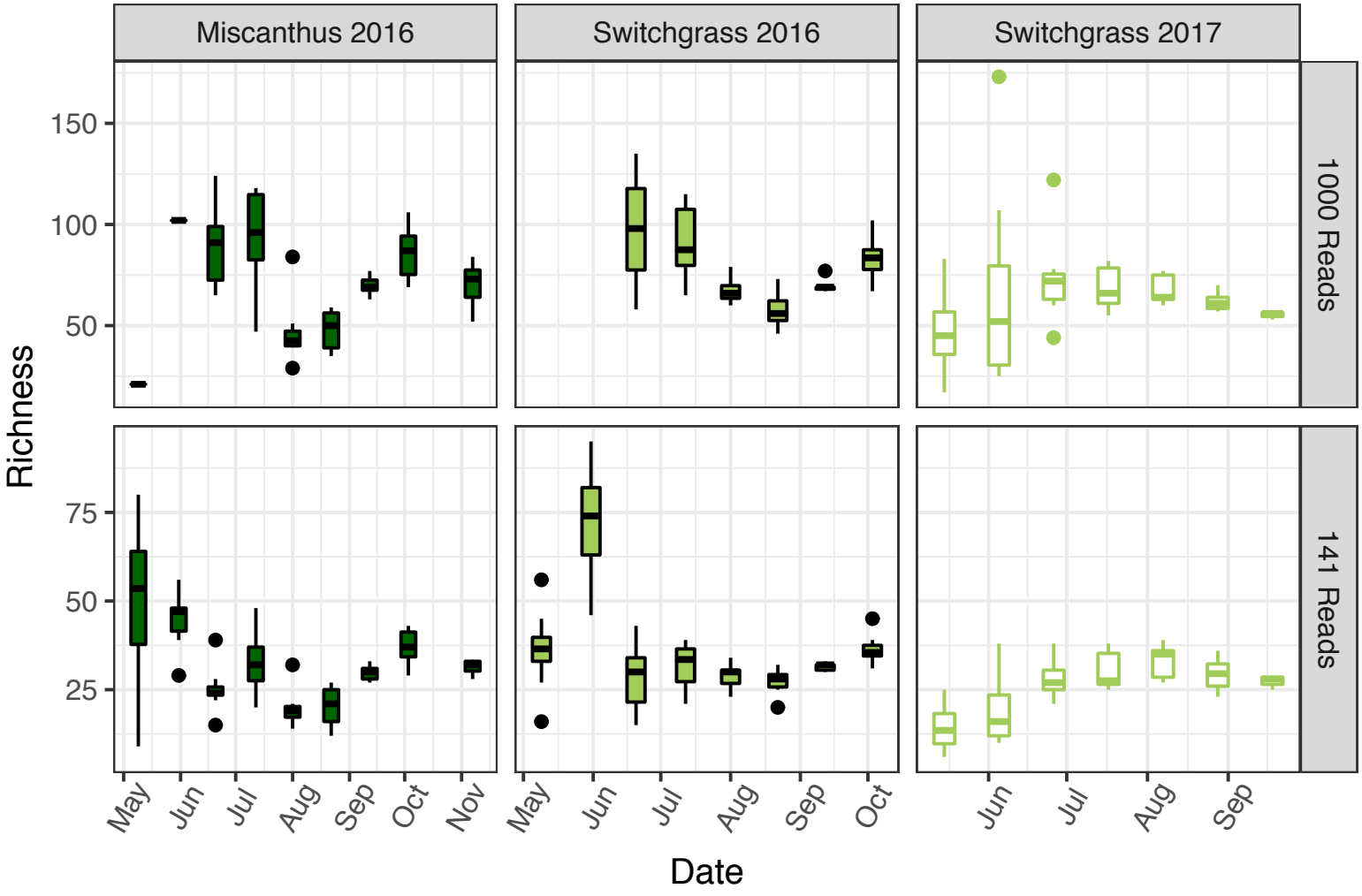
Miscanthus 2016
Switchgrass 2016
Switchgrass 2017
1000 Reads
141 Reads
Richness
150
100
50
75
50
25
May
Jun
Jul
Aug
Sep
Oct
Nov
May
Jun
Jul
Aug
Sep
Oct
Jun
Jul
Aug
Sep
Date

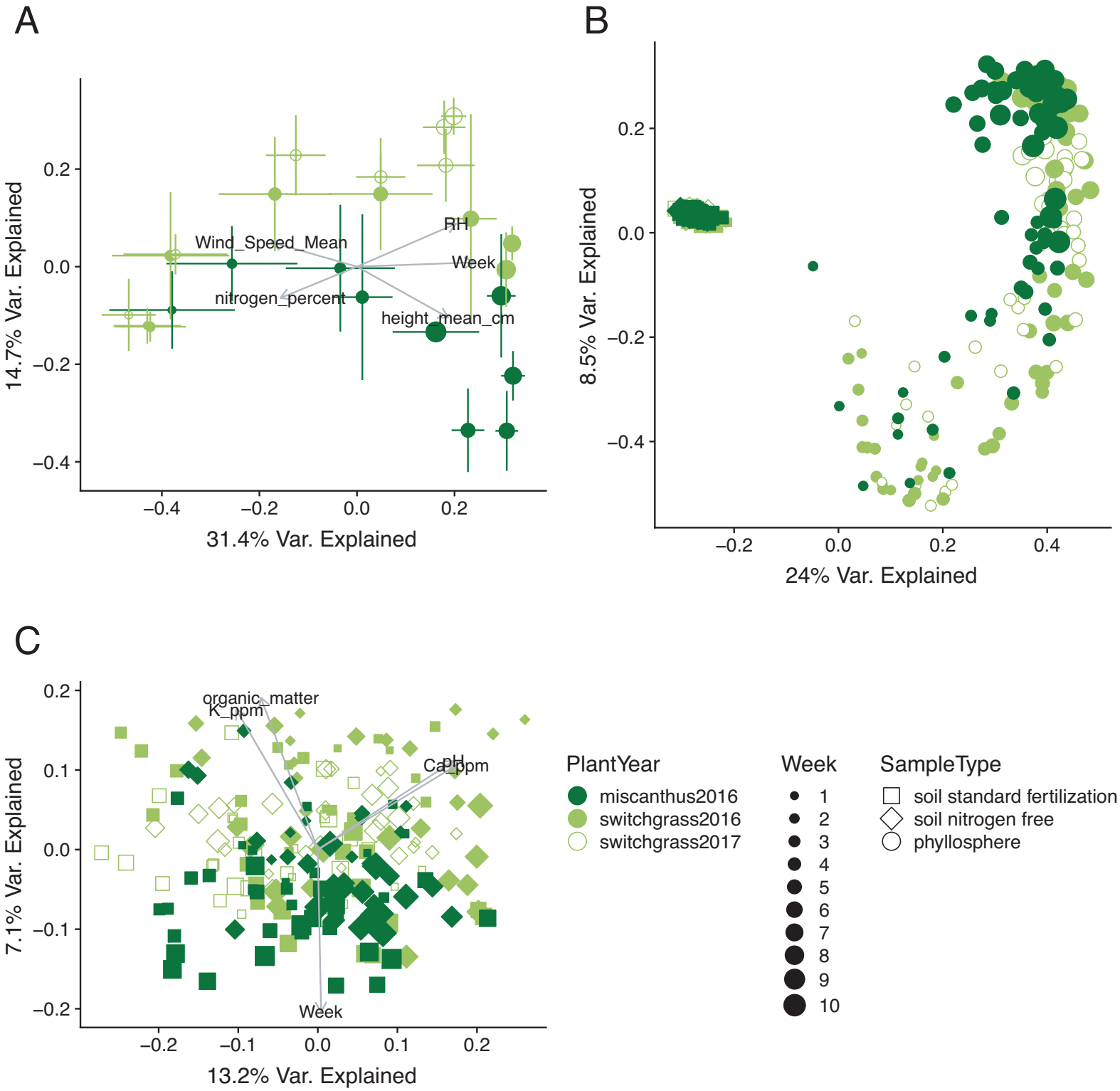
A
Wind_Speed_Mean
RH
Week
nitrogen_percent
height_mean_cm
14.7% Var. Explained
31.4% Var. Explained
B
8.5% Var. Explained
24% Var. Explained
C
organic_matter
K_ppm
pH
Ca_ppm
Week
7.1% Var. Explained
13.2% Var. Explained
PlantYear
miscanthus2016
switchgrass2016
switchgrass2017
Week
1
2
3
4
5
6
7
8
9
10
SampleType
soil standard fertilization
soil nitrogen free
phyllosphere

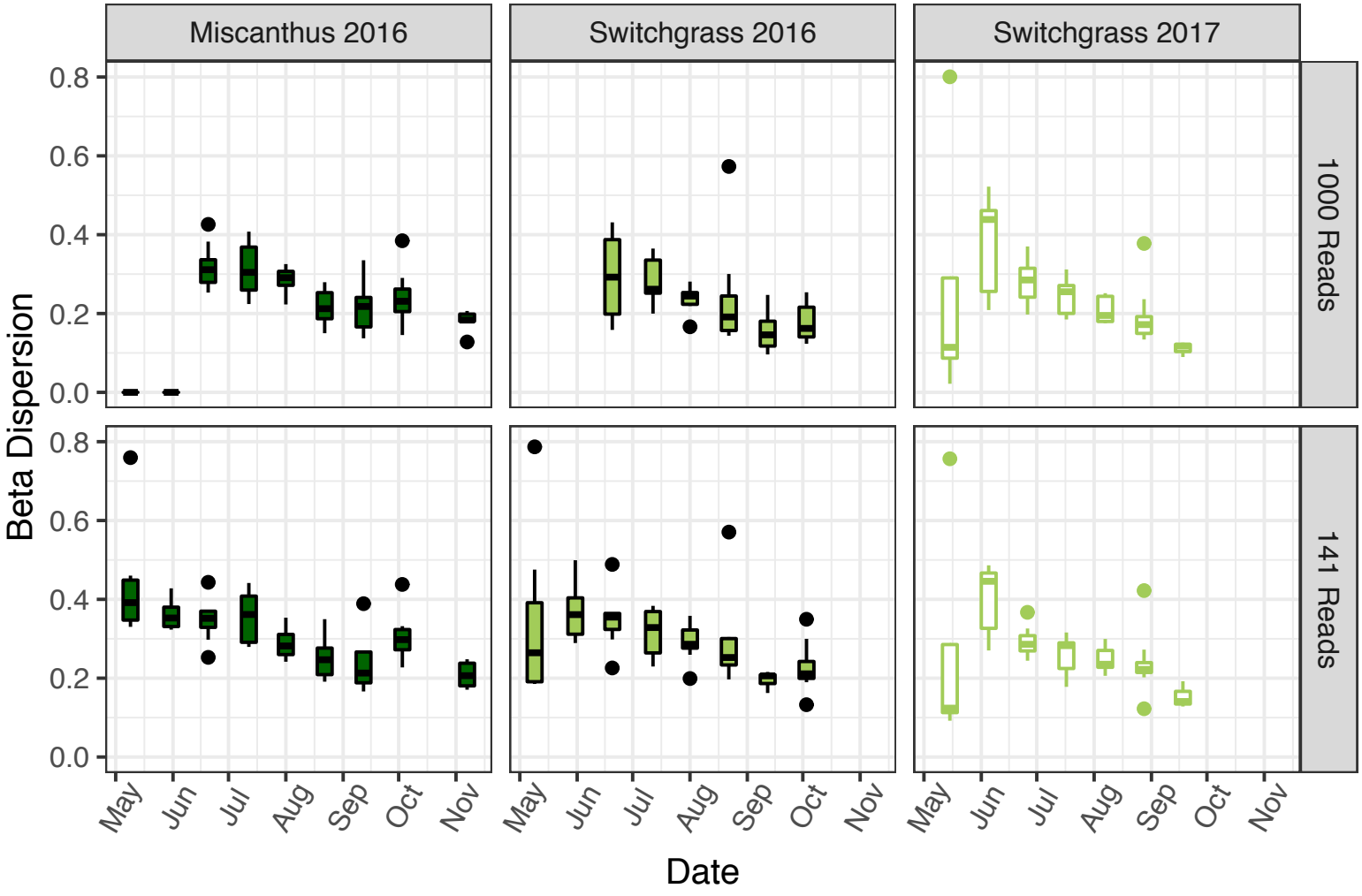
Miscanthus 2016
Switchgrass 2016
Switchgrass 2017
1000 Reads
141 Reads
Beta Dispersion
0.0
0.2
0.4
0.6
0.8
May
Jun
Jul
Aug
Sep
Oct
Nov
Date

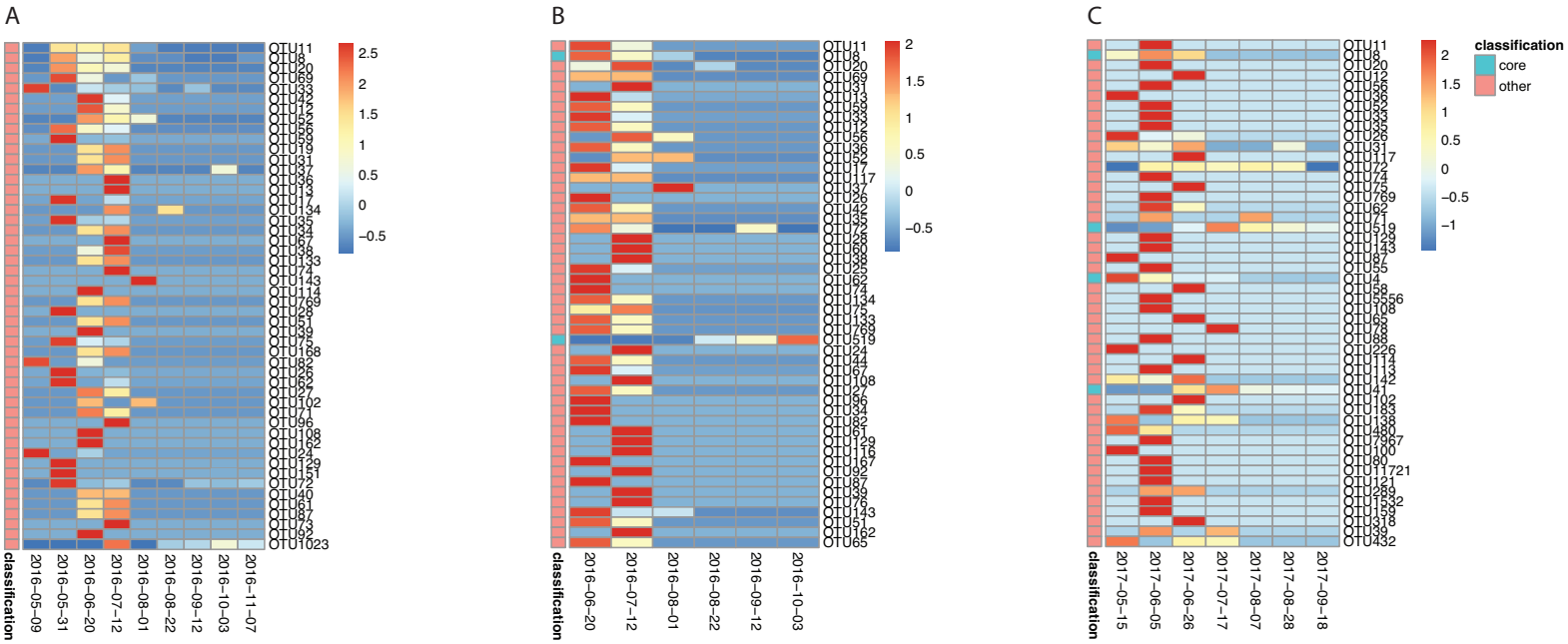
A
B
C
classification
core
other
2016–05–09
2016–05–31
2016–06–20
2016–07–12
2016–08–01
2016–08–22
2016–09–12
2016–10–03
2016–11–07
2017–05–15
2017–06–05
2017–06–26
2017–07–17
2017–08–07
2017–08–28
2017–09–18

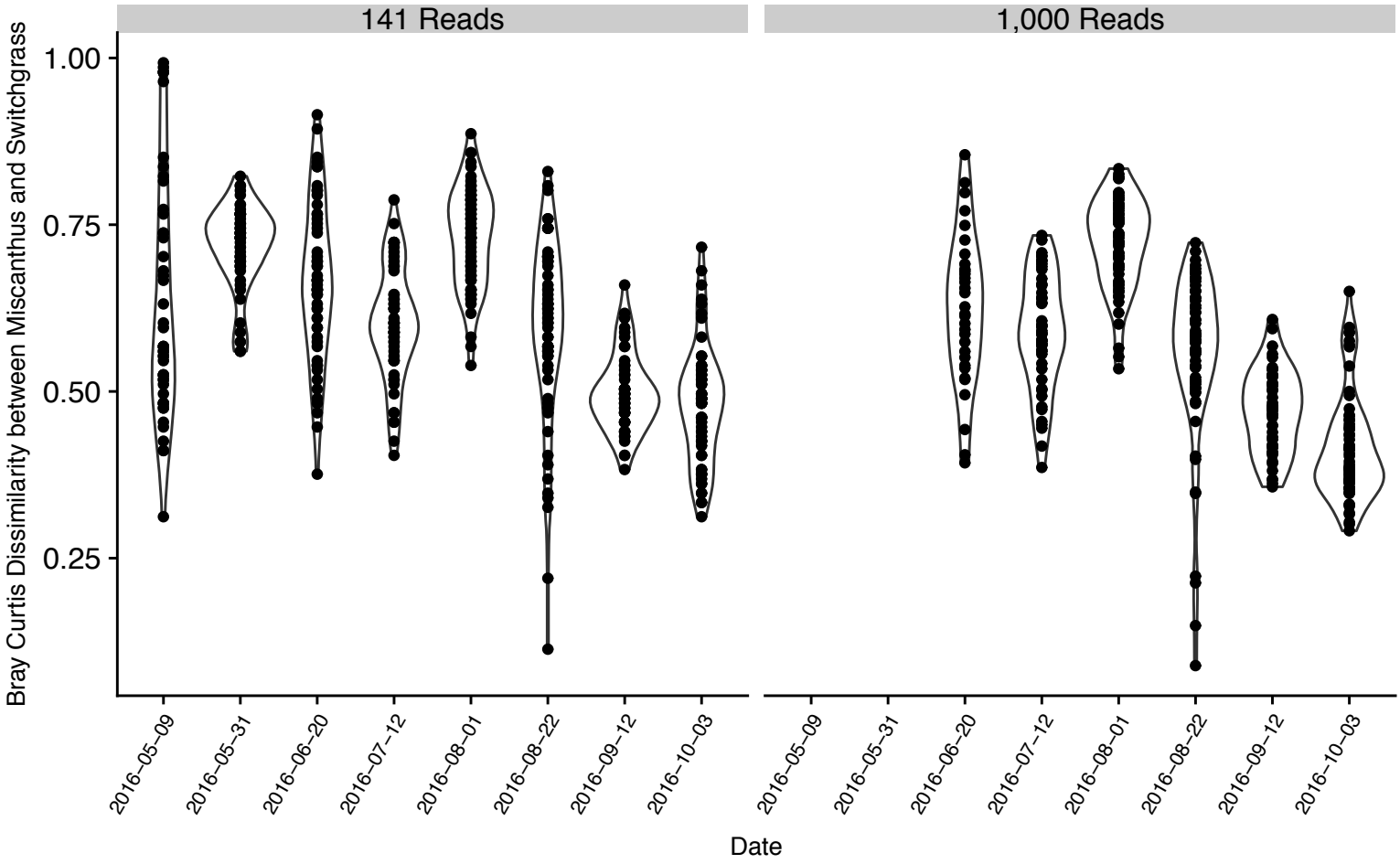
141 Reads
1,000 Reads
Bray Curtis Dissimilarity between Miscanthus and Switchgrass
1.00
0.75
0.50
0.25
2016–05–09
2016–05–31
2016–06–20
2016–07–12
2016–08–01
2016–08–22
2016–09–12
2016–10–03
Date

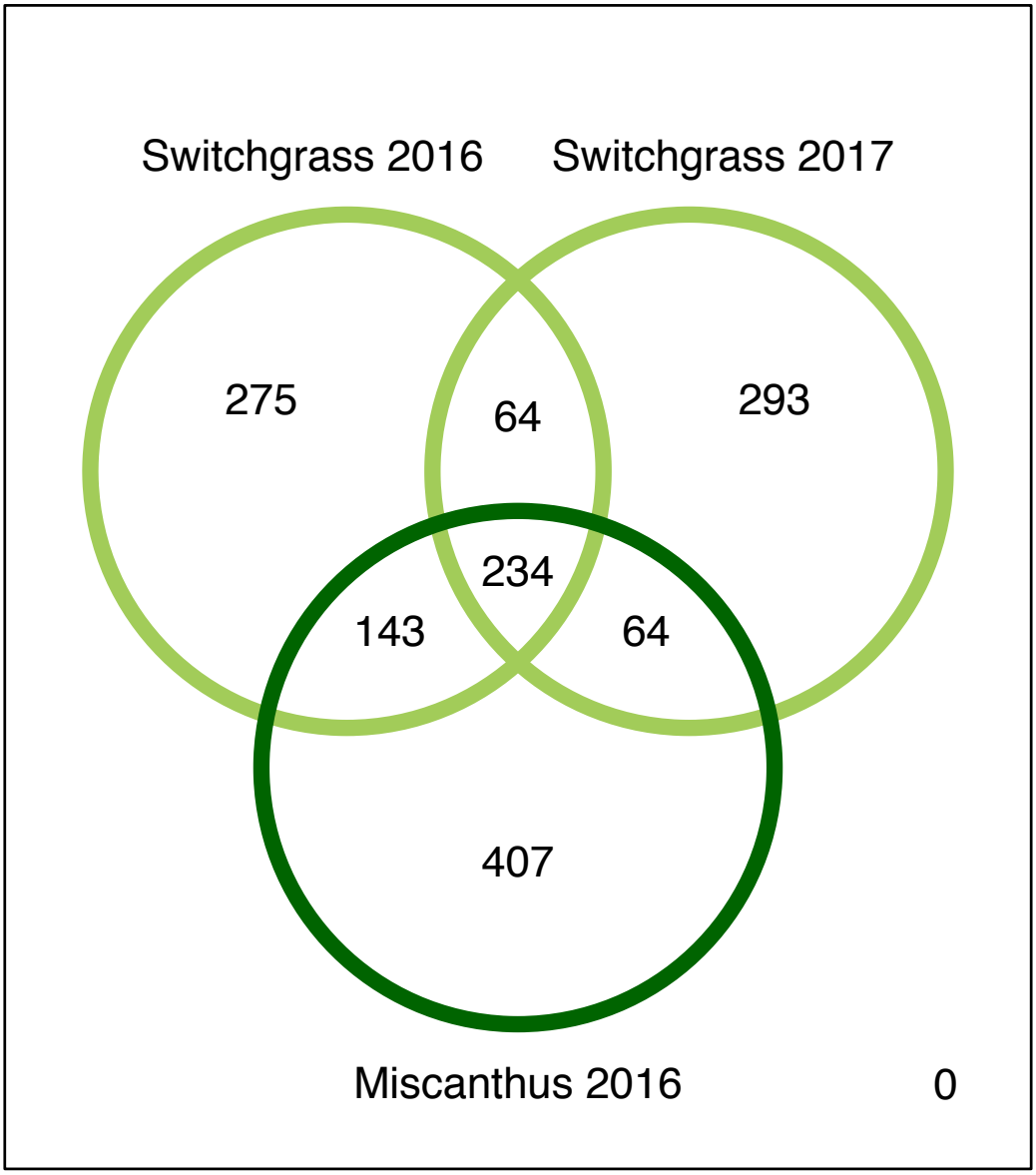
Switchgrass 2016
Switchgrass 2017
275
64
293
234
143
64
407
Miscanthus 2016
0

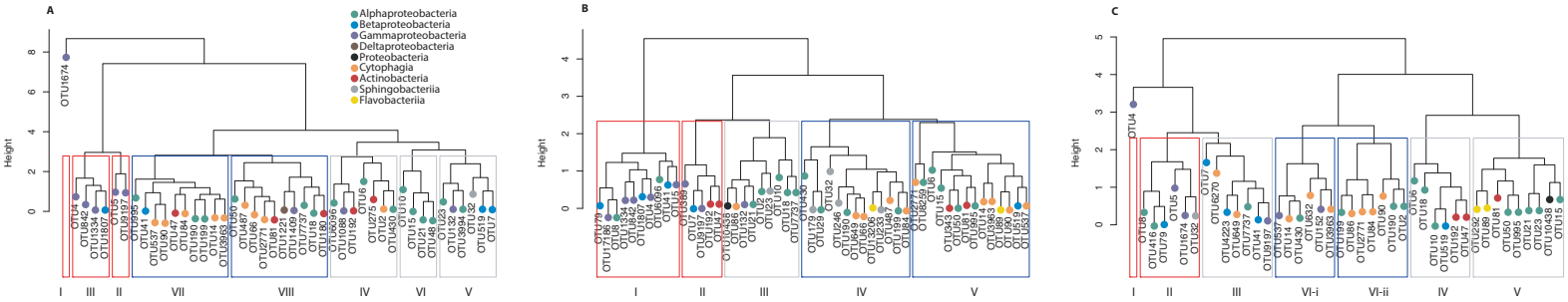
A
Alphaproteobacteria
Betaproteobacteria
Gammaproteobacteria
Deltaproteobacteria
Proteobacteria
Cytophagia
Actinobacteria
Sphingobacteriia
Flavobacteriia
Height
OTU1674
I
III
II
VII
VIII
IV
VI
V
B
Height
I
II
III
IV
V
C
Height
OTU4
I
II
III
VI-i
VI-ii
IV
V

Table S1. **Sequencing summary of phyllosphere microbial communities characterized in this study**, categorized by crop and year. QC is quality controlled.

	Miscanthus 2016	Switchgrass 2016	Switchgrass 2017
Raw Read Pairs	7336923	7120682	9271169
QC Reads	7142900	6883631	7123783
% Chloroplast/ Mitochondria of QC Reads	77.27%	67.16%	12.32%
Samples >= 141 Reads	65	62	44
Samples >= 1,000 Reads	53	43	44
Samples >= 10,000 Reads	36	27	44
OTUs (rarefied to 141 Reads)	540	685	232
OTUs (rarefied to 1,000 Reads)	1010	859	769
OTUs (rarefied to 10,000 Reads)	1121	896	2320

Table S2. **Comparison of overarching patterns of beta diversity across the same dataset rarefied to different sequencing depths**. We compared all pairs of 141, 500, 1000, 5000, or 10000 reads per sample. All tests were significant at $p < 0.001$ on 1000 permutations.

	141 Reads	500 Reads	1000 Reads	5000 Reads
500 Reads	0.932			
1000 Reads	0.872	0.982		
5000 Reads	0.752	0.931	0.976	
10000 Reads	0.725	0.916	0.967	0.999

Table S3. Fitted environmental variables that explain changes in microbiome community structure. All are $p < 0.05$ unless designated as not significant (NS). Values in bold (EnvFit $R^2 > 0.40$) were plotted as vectors in **Figure 2**.

Variable Tested	Axis 1	Axis 2	R squared	P -value
precipitation	-0.127	0.146	0.038	0.703
Air_temp_mean	-0.298	-0.078	0.095	0.384
air_temp_max	-0.212	-0.056	0.048	0.633
Air_Temp_Min	-0.242	0.139	0.078	0.439
Air_Pressure	-0.022	0.217	0.048	0.653
RH	0.474	0.444	0.422	0.008
AH	-0.081	0.102	0.017	0.834
Wind_Speed_Mean	-0.703	-0.213	0.539	0.001
Solar_Radiation	-0.258	-0.368	0.202	0.118
PAR	-0.300	-0.288	0.173	0.162
soil_temp_5_cm_bare_avg	-0.408	-0.061	0.170	0.163
Week	0.730	0.356	0.659	0.001
LDMC_mg_per_g	0.418	0.177	0.206	0.001
nitrogen_percent	-0.392	-0.416	0.327	0.001
carbon_percent	0.345	0.038	0.121	0.001
carbon_per_nitrogen	0.274	0.134	0.093	0.003
height_mean_cm	0.730	-0.230	0.586	0.001
pH	-0.027	0.219	0.049	0.047
P_ppm	-0.120	-0.097	0.024	0.187
K_ppm	-0.445	0.187	0.233	0.001
Ca_ppm	0.047	0.059	0.006	0.659
Mg_ppm	-0.366	-0.125	0.149	0.001
organic_matter	-0.348	-0.036	0.123	0.001
NO3N_ppm	0.003	-0.080	0.006	0.646
NH4_ppm	-0.461	0.090	0.220	0.001
soil_moisture_percent	0.609	0.015	0.371	0.001
soil_temp_10cm	-0.364	-0.028	0.133	0.001